Biosensors and Bioelectronics 26 (2011) 2252–2257

Contents lists available at ScienceDirect

Biosensors and Bioelectronics

journal homepage: www.elsevier.com/locate/bios

Enhanced direct electrochemistry of glucose oxidase and biosensing for glucose via synergy effect of graphene and CdS nanocrystals

Kun Wang*, Qian Liu, Qing-Meng Guan, Jun Wu, He-Nan Li, Jia-Jia Yan

Key Laboratory of Modern Agriculture Equipment and Technology, School of Chemistry and Chemical Engineering, Jiangsu University, 301 Xuefu Road, Zhenjiang 212013, Jiangsu, PR China

ARTICLE INFO

Article history:
Received 1 August 2010
Received in revised form
20 September 2010
Accepted 21 September 2010
Available online 29 September 2010

Keywords:
Direct electrochemistry
Glucose oxidase
Synergy effect
Graphene
CdS nanocrystal

ABSTRACT

Integrating graphene-based composites with enzyme provides a potent strategy to enhance biosensor performance due to their unique physicochemical properties. Herein we report on the utilization of graphene–CdS (G–CdS) nanocomposite as a novel immobilization matrix for the enzymes, which glucose oxidase (GOD) was chosen as model enzyme. In comparison with the graphene sheet and CdS nanocrystal, G–CdS nanocomposite exhibited excellent electron transfer properties for GOD with the rate constant (k_s) of 5.9 s^{-1} due to the synergy effect of graphene sheet and CdS nanocrystals. Further, based on the decrease of the electrocatalytic response of the reduced form of GOD to dissolved oxygen, the obtained glucose biosensor displays satisfactory analytical performance over an acceptable linear range from 2.0 to 16 mM with a detection limit of 0.7 mM, and also prevents the effects of interfering species, which is suitable for glucose determination by real samples. These results mean that this immobilization matrix not only can be used for immobilizing GOD, but also can be extended to other enzymes and bioactive molecules, thus providing a promising platform for the development of biosensors.

1. Introduction

Graphene, a monolayer of sp^2 hybridized carbon atoms packed into a dense honeycomb crystal structure (Allen et al., 2010), has received increasing attention during recent years because of several breakthroughs in fundamental research and promising practical applications. Due to its unique physicochemical properties including high surface area (Li et al., 2008), excellent electric conductivity (Geim and Novoselov, 2007), strong mechanical strength, ease of functionalization and mass production (Shao et al., 2010), it has shown great promise in many applications, such as supercapacitors (Stoller et al., 2008), batteries (Guo et al., 2009; Wang et al., 2009a), solar cells (Wang et al., 2008), pH sensors, etc. (Ang et al., 2008). Recently, biological and electrocatalytic applications of graphene have also started to be concerned by virtue of its excellent electrocatalytic ability (Wang et al., 2009b). Based on previous reports, graphene-based electrodes have been applied in the electrochemical stripping determination of cadmium (Li et al., 2009a), the selective detection of dopamine (Wang et al., 2009c; Kim et al., 2010), and a platform for electrocatalytic oxidation of hydrazine in alkaline media (Wang et al., 2010a). In the meantime, recent studies exhibit the special properties of graphene may provide insight to fabricate novel biosensors for virtual applications: the high surface area is helpful in increasing the surface loading of the target enzyme molecules on the surface, the excellent conductivity and small band gap are favorable for conducting electrons from the biomolecules (Stankovich et al., 2006), and graphene-based chemical sensors can also have a much higher sensitivity because of the low electronic noise from thermal effect (Ao et al., 2008). Wu's group achieved the direct electron transfer of cytochrome *c* on the cytochrome *c*/graphene-based electrode, which indicated graphene was biocompatible and suitable for biomedical applications (Wu et al., 2010). Lin and co-workers studied the electrochemical behavior of glucose oxidase (GOD) at a graphene–chitosan modified electrode, which demonstrated the direct electron transfer of GOD (Kang et al., 2009). These results indicate graphene shows a grand potential for fabricating electrochemical sensing interface, and up to now, it is just the beginning of this fantastic topic.

Moreover, it will be attractive to prepare carbon-based hybrid composites, because such functionalized materials may generate synergy effect and thus enhance their performance in sensing applications (Wu et al., 2009). For example, coupling carbon nanotubes (CNTs) with CdTe quantum dots resulted in facilitating direct electron transfer processes and retaining the good bioactivity of GOD via synergy effect (Liu et al., 2007). Yang et al. have showed the synergy effect between CNTs and cobalt hexacyanoferate nanoparticles (CoNP) with the significant improvement of redox activity of CoNP (Yang et al., 2006). Zou's report has also showed the

* Corresponding author. Tel.: +86 511 8791800; fax: +86 511 8791708.
E-mail address: wangkun@ujs.edu.cn (K. Wang).

0956-5663/$ – see front matter © 2010 Elsevier B.V. All rights reserved.
doi:10.1016/j.bios.2010.09.043

polyaniline-prussian blue/multi-walled CNTs system shows synergy effect which amplified the H_2O_2 sensitivity greatly (Zou et al., 2007). Further, Niu and co-workers indicated the PVP-protected graphene/polyethylenimine-functionalized ionic liquid nanocomposite exhibits good electrocatalysis toward the reduction of H_2O_2, and further achieved the direct electron transfer of GOD (Shan et al., 2009). Based on the electrocatalytic synergy effect between functionalized graphene sheets and metal nanoparticles (such as Au, Pt) to H_2O_2 and O_2, glucose biosensors with good responses were successfully achieved (Wu et al., 2009; Shan et al., 2010).

In the meantime, semiconductor nano-sized CdS showed potential applications in protein electrochemistry due to its remarkable physicochemical properties. It is noted that CdS nanoparticles were used to incorporate with GOD for realizing the direct electron transfer, and CdS has been found efficiently enhancing the electron transfer reactivity of GOD (Huang et al., 2005). Moreover, CdS hollow nanospheres have recently been used in immobilizing hemoglobin and the direct electron transfer has been obtained (Dai et al., 2008). It has been reported that the integration of graphene and metal nanoparticles offer synergy effects in electrocatalytic applications (Wu et al., 2009; Shan et al., 2010), so we have reasons to expect the nanocomposite of graphene and CdS nanocrystals (NCs) has the same effect, which has not been reported as far as we know.

Herein, in order to explore the distinct advantages of graphene–CdS (G–CdS) nanocomposite in enzyme adsorption and bioactivity, GOD was chosen as a model enzyme and the direct electron transfer of the immobilized GOD was investigated. Due to the synergy effect between CdS NCs and graphene, the fabricated electrode showed excellent electrochemical behavior and the direct electron transfer between the GOD and the modified electrode was easily achieved, indicating G–CdS nanocomposite could be a good candidate material for immobilizing biomolecules and fabricating the third-generation biosensors.

2. Experimental

2.1. Reagents

Glucose oxidase (GOD, from *Aspergillus niger*, EC 1.1.3.4, 35.3 U/mg), β-D-(+)-glucose and Nafion (5 wt% solution) were purchased from Sigma Chemical (USA). The stock GOD solution was prepared in the 0.05 M phosphate buffer solution (PBS, pH 7.4) and stored at 4 °C. D-Glucose solution (0.1 M) was prepared and allowed to mutarotate at room temperature overnight before use. G–CdS nanocomposite with the graphene content of 4.6% was synthesized according to the method described in our previous work (Wang et al., 2010b). PBS (0.05 M) of various pH values were prepared by mixing stock standard solutions of NaH_2PO_4 and Na_2HPO_4, and adjusting the pH with 0.05 M H_3PO_4 or NaOH. All other chemicals were of analytical grade and used without further purification, and all solutions were prepared with doubly distilled water.

2.2. Apparatus

Transmission electron microscopy (TEM) images were taken with a JEOL 2100 transmission electron microscopy (JEOL, Japan) operated at 200 kV. The Fourier transform infrared (FTIR) spectra of the samples were obtained from Nicolet Nexus 470 FTIR Spectrometer (Thermo Nicolet, USA). Electrochemical impedance measurements were performed in a 0.1 M KCl solution containing 5 mM $K_3[Fe(CN)_6]/K_4[Fe(CN)_6]$ with a frequency range from 0.01 Hz to 10 kHz at 0.23 V, and the amplitude of the applied sine wave potential in each case was 5 mV. The electrochemical experiments were performed with a CHI660 B electrochemical analyzer (Chen Hua Instruments, Shanghai, China). All experiments were carried out at room temperature (ca. 25 °C) with a conventional three-electrode system where glassy carbon electrode was used as working electrode, Ag/AgCl (saturated KCl solution) as reference electrode and platinum wire as counter electrode, respectively. Electrolyte solutions were purged with high-purity nitrogen for at least 20 min prior to experiments, and solutions in the cell were kept under a nitrogen atmosphere.

2.3. Preparation of modified electrodes

Prior to modification, the GCE (3 mm in diameter) was first polished with sand paper followed by 1.0, 0.3, and 0.05 μm alumina slurry, respectively. After successive sonication in ethanol and double distilled water, the electrode was rinsed with double distilled water and allowed to dry at room temperature. The modified electrode was prepared by a simple casting method. 2.2 mg mL^{-1} G–CdS suspension was prepared by dispersing 1.1 mg G–CdS nanocomposite in 0.5 mL ethanol with ultrasonic agitation for about 2 min. To accomplish the preparation of G–CdS–GOD/GC electrode, firstly, the as-prepared G–CdS suspension and 30 μL of 5% Nafion were mixed with ultrasonic agitation for 2 min; secondly, the suspension was mixed thoroughly with 23 μL of 22 mg mL^{-1} GOD which solubilized in pH 7.4 PBS. Then, about 6 μL of this suspension was cast on the pretreated GCE surface and dried at 4 °C to form G–CdS–GOD modified GCE (denoted as G–CdS–GOD/GCE). Finally, the modified GCE was immersed in 0.05 M PBS (pH 7.4) to remove the loosely adsorbed GOD and was stored at 4 °C in a refrigerator under dry conditions when not use. For comparison, G–CdS/GCE, CdS–GOD/GCE and graphene–GOD/GCE with the same quantities of GOD were prepared using the similar procedure.

3. Results and discussion

3.1. Transmission electron microscopy image and FTIR spectra

The morphology of G–CdS nanocomposite was characterized by transmission electron microscopy (TEM). Fig. 1A shows TEM image of G–CdS nanocomposite, revealing that the G–CdS consisted of 2D graphene sheets decorated with CdS NCs (Cao et al., 2009). And the individual CdS NCs with an average diameter of 12 nm are well separated from each other and well spread out on the graphene sheets.

We conducted a preliminarily investigation into the structural changes of GOD immobilized on G–CdS nanocomposite by using FTIR spectroscopy, as shown in Fig. 1B. The pure G–CdS nanocomposite exhibits absorption bands at 1601 and 1069 cm^{-1}, which correspond to the deformation vibration of H–O–H bonds from the adsorbed water (Bao et al., 2008). The spectra for pure GOD molecules is characterized by two absorption bands centered at 1653 and 1529 cm^{-1}, which are the typical amide I and amide II absorption bands of protein molecules, respectively (Wang et al., 2009a,b,c). After being adsorbed on G–CdS nanocomposite, only slight shifts of the amide I (from 1653 to 1643 cm^{-1}) and amide II (from 1529 to 1523 cm^{-1}) peaks of GOD were observed, confirming that GOD is effectively immobilized on the G–CdS nanocomposite (Bao et al., 2008). Further, the retention of this absorption band indicates that the interactions between the G–CdS and the GOD molecules do not change the spatial structure of the protein during the immobilization process (Wu et al., 2007; Zhao et al., 2010).

3.2. Electrochemical impedance spectroscopy (EIS)

The EIS measurements can give information on the impedance changes of the electrode surface during the modification process. The Nyquist plot of impedance spectra includes a semicircle portion

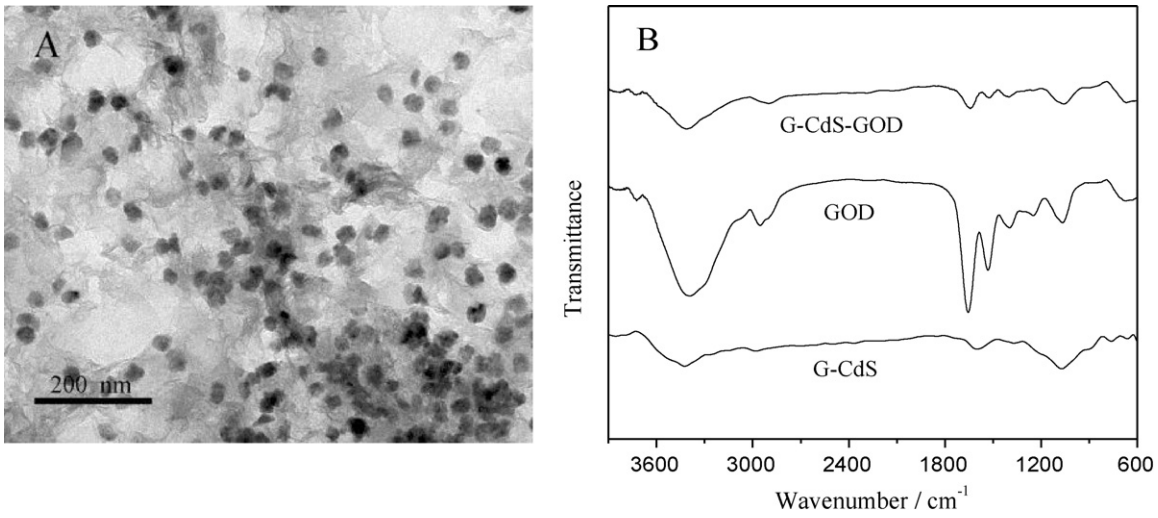

Fig. 1. (A) TEM image of G–CdS nanocomposite and (B) FTIR spectra of G–CdS nanocomposite, pure GOD and GOD-loaded G–CdS.

and a linear portion. The semicircular portion at higher frequencies corresponds to the electron-transfer-limited process and its diameter is equal to the electron-transfer resistance, which controls the electron-transfer kinetics of the redox probe at the electrode interface. Meanwhile, the linear part at lower frequencies corresponds to the diffusion process (Kang et al., 2009). Fig. 2 exhibits the impedance spectroscopy of different modified electrodes in the presence of equimolar $Fe(CN)_6^{3-/4-}$ ions, respectively. The diameter of Nyquist circle on bare GCE was extremely small, indicating that the charge transfer at bare electrode was relatively facile. After Nafion was coated on the electrode, a substantial increase in the diameter of the semicircle was observed. The reason is that the Nafion could act as the inert electron and mass transfer blocking layer, and it hinders the diffusion of ferricyanide toward the electrode surface (Liu et al., 2006). When G–CdS nanocomposite was added into Nafion film, the diameter of Nyquist circle decreased dramatically, indicating G–CdS nanocomposite could act as a good electron-transfer interface between the EIS probe and the electrode (Deng et al., 2009). At last, when GOD was absorbed into the G–CdS nanocomposite film, we found that the diameter of the Nyquist circle decreased, which was due to the direct electron transfer between the GOD molecules and the electrode (Liu et al., 2006), also confirming that the GOD was successfully immobilized on the composite film.

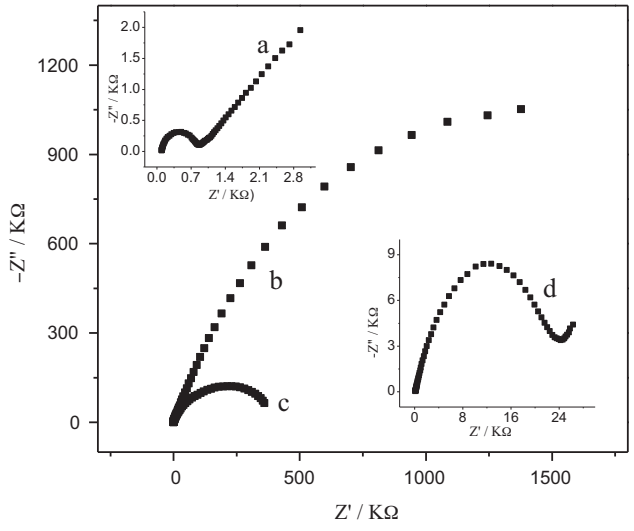

Fig. 2. Electrochemical impedance spectra of bare GCE (a), Nafion/GCE (b), G–CdS/GCE (c) and G–CdS–GOD/GCE (d) in 0.1 M KCl containing 5 mM $K_3[Fe(CN)_6]/K_4[Fe(CN)_6]$.

3.3. Direct electrochemistry of GOD immobilized in the G–CdS film

Cyclic voltammogram was employed to evaluate the performance of the fabricated biosensor during stepwise modification. The direct electrochemistry of GOD immobilized on the modified GCE was investigated in 0.05 M nitrogen-saturated PBS (pH 7.4). As shown in Fig. 3A, the cyclic voltammogram of G–CdS–GOD/GCE shows a pair of well-defined and nearly reversible redox peaks at −0.327 V and −0.343 V with the peak-to-peak separation (ΔE_p) of 16 mV at 50 mV s^{-1} (Fig. 3A, curve c), revealing a fast electron transfer process (Liu et al., 2007). In contrast, no peak is observed at bare GCE and G–CdS/GCE, which indicates they are electrochemically silent in this potential window. Therefore, the redox peaks at G–CdS–GOD/GCE are attributed to the direct electron transfer of GOD for the conversion of GOD(FAD) to GOD($FADH_2$), moreover, the formal potential of the GOD modified electrode, calculated from the average value of the anodic and cathodic peak potentials, is about −0.335 V (vs. Ag/AgCl), indicating the G–CdS nanocomposite plays an important role in facilitating the electron exchange between the electroactive center of GOD and the modified electrode. In addition, compared to G–CdS–GOD modified electrode, graphene–GOD and CdS–GOD film also offer a weak electrochemical reaction for the GOD (Fig. 3B, curves a and b), which can be expected that graphene and CdS NCs efficiently realize the direct electron transfer between the GOD's electroactive center and the electrode. Moreover, the quantities of GOD are equal in the films and the current of G–CdS–GOD/GCE was larger than the sum current of the graphene–GOD and CdS–GOD modified electrodes, indicating the combination of graphene and CdS NCs improved the electronic transport capacity of the electrode and the presence of synergy effect in G–CdS–GOD film.

Based on these, the effect of scan rate on the voltammetric response of immobilized GOD has also been investigated. As shown in Fig. S1A, with the scan rate increasing, the cathodic and anodic peak currents increased simultaneously in 0.05 M PBS (pH 7.4). The peak separation (ΔE_p) ranged from 16 mV to 35 mV with the scan rate increasing from 10 to 300 mV s^{-1}, possibly because of the resistance of the modified layer (Bao et al., 2008). The small ΔE_p value indicated the faster direct electron transfer between the redox-

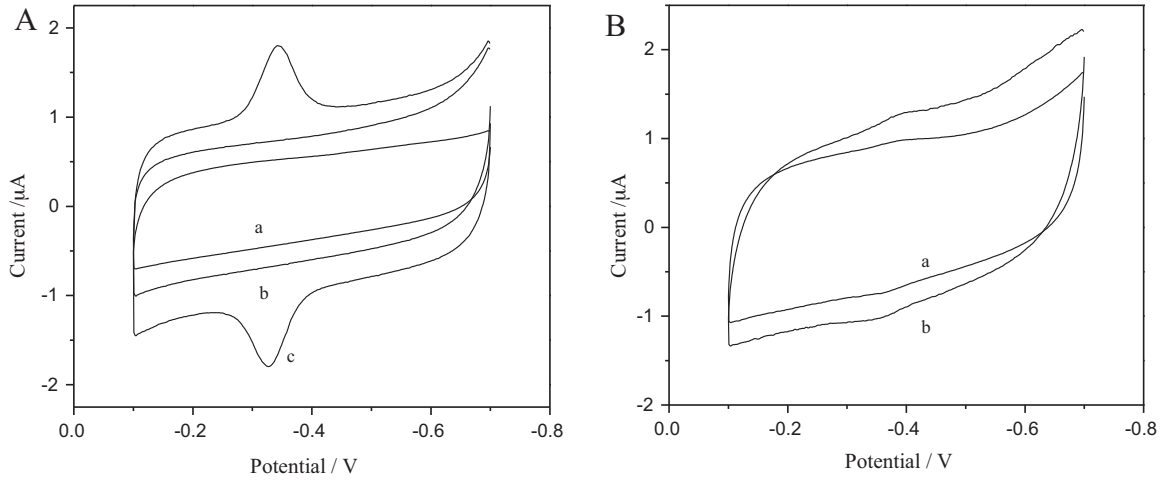

Fig. 3. (A) Cyclic voltammograms of bare GCE (a), G–CdS/GCE (b) and G–CdS–GOD/GCE (c) in 0.05 M nitrogen-saturated PBS (pH 7.4) at 50 mV s^{-1}. (B) Cyclic voltammograms of graphene–GOD/GCE (a) and CdS–GOD/GCE (b) in 0.05 M nitrogen-saturated PBS (pH 7.4) at 50 mV s^{-1}.

active site of GOD (the cofactor FAD) and the GCE without the help of electron transfer mediator (Deng et al., 2009), and the good linear relationship (R^2 = 0.999) between the peak currents and the scan rates (Fig. S1A inset) indicate that the redox process of the prepared biocomposite is surface-confined (Liu and Ju, 2003). The electron transfer rate (k_s) between the GOD and the electrode is calculated as 5.9 s^{-1} according to the equation of $k_s = mnFv/RT$, when the peak-to-peak separation is less than 200 mV (Laviron, 1979), where m is a parameter related to the peak-to-peak separation, n is the number of electrons, v is the scan rate, and T is the temperature. This value is much larger than 1.28 s^{-1} and 1.56 s^{-1} for GOD immobilized on graphene and CdS NCs modified electrode alone, indicating the presence of synergy effect in G–CdS–GOD film, which is accordance with the cyclic voltammetric performances of various GOD modified electrodes (shown in Fig. 3). In addition, it is much larger than the corresponding values observed for GOD immobilized on graphene–chitosan (2.83 s^{-1}) (Kang et al., 2009), MWCNTs–chitosan (1.08 s^{-1}) (Luo et al., 2006), SWCNTs–chitosan (3.0 s^{-1}) (Zhou et al., 2008a), porous TiO_2 (3.96 s^{-1}) (Bao et al., 2008), boron-doped MWCNTs (1.56 s^{-1}) (Deng et al., 2008) and CNTs–poly(diallyldimethylammonium chloride) (PDDA) (2.76 s^{-1}) (Wen et al., 2007) modified electrode. The significant increase in the electron transfer rate further proved that the G–CdS nanocomposite can facilitate the electron transfer between the redox-active sites of enzyme and the electrode (Deng et al., 2009).

It is well known that the direct electrochemistry of GOD is a two-electron coupled with two-proton reaction and therefore, peak potentials should be pH-dependent (Li et al., 2008). Fig. S1B shows cyclic voltammograms of the G–CdS–GOD modified electrode in 0.05 M PBS with different pH values. In each pH solution, a pair of stable and well-defined reversible redox peaks of the GOD is observed. Furthermore, negative shifts in both anodic and cathodic peak potentials are observed with increasing pH value from 5.0 to 8.0, which indicates that the hydrogen ion is involved in the electrode reaction of GOD. This result is in agreement with previous reports (Deng et al., 2008; Zhao et al., 2006; Wang et al., 2009a,b,c; Huang et al., 2005), and the maximum current response is occurred at pH 7.4. In addition, the formal potential has a linear relationship with pH from 5.0 to 8.0 with a slope of −58.3 mV/pH (Fig. S1B inset), which is very close to the theoretical value of −58.6 mV/pH (Liu et al., 2005) for a reversible coupled with two-proton and two-electron transfer electrochemical process. All of these indicate that two protons ($2H^+$) and two electrons ($2e^-$) maybe participate in the direct electrochemical reaction of GOD immobilized.

3.4. Detection of glucose based on direct electrochemistry at G–CdS–GOD modified electrode

In order to show the enzymatic activity of GOD immobilized on the modified electrode, further electrocatalytic experiments about the reaction of oxygen and glucose to GOD were carried out. Fig. 4 shows the cyclic voltammograms of the G–CdS–GOD/GCE in 0.05 M PBS (pH 7.4) without and with glucose at a scan rate of 50 mV s^{-1}. An increase in cathodic peak current and decrease in anodic peak current were observed in the air-free and O_2-saturated solutions in the absence of glucose as compared to the corresponding peaks in the nitrogen-saturated solution. This is because the electrochemically formed GOD($FADH_2$) electrocatalyzed the reduction of oxygen. Moreover, with addition of glucose to oxygen-saturated PBS, the reduction current decreased. The higher glucose concentration was, the more reduction current decreased. It can be attributed to the fact that adding glucose triggers the enzyme-catalysis reaction of GOD and glucose, decreasing the GOD's oxidized form on the G–CdS–GOD/GCE, and thus decreasing the electrode reduction current (Liu et al., 2007).

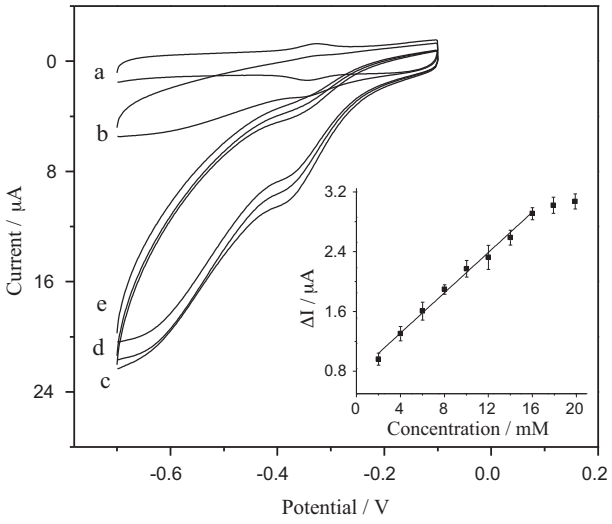

Fig. 4. Cyclic voltammograms of G–CdS–GOD/GCE in nitrogen-saturated (a), air-free (b), oxygen-saturated 0.05 M pH 7.4 PBS in the absence (c) and presence of 2.0 mM (d), 4.0 mM (e) glucose at 50 mV s^{-1}. Inset: calibration curve for glucose sensing.

Since the determination of glucose is of great important in the biological, clinical and food fields, the G–CdS–GOD/GCE was further used as a glucose biosensor, which based on the decrease of the electrocatalytic response to dissolved oxygen. As shown in Fig. 4 inset, the biosensor exhibited an acceptable linear response to glucose in the concentration range of 2.0–16 mM (R^2 = 0.996) with a detection limit of 0.7 mM (S/N = 3). This linear range is comparable to that of 2–10 mM for the immobilization of GOD on graphene/AuNPs/chitosan nanocomposites film (Shan et al., 2010) and 2–14 mM for GOD on the graphene–GOD–PFIL matrix (Shan et al., 2009). It is well known that the diabetic glucose concentration is above 7.0 mM (Li et al., 2009b), which indicates that the as-prepared biosensor is suitable for its practical application for the determination of human blood sugar concentration without sample pretreatment. Furthermore, the sensitivity of the as-prepared biosensor was calculated to be 1.76 $\mu A\,mM^{-1}\,cm^{-2}$, which was higher than 1.06, 0.2 and 0.053 $\mu A\,mM^{-1}\,cm^{-2}$ for the glucose biosensors based on single-walled carbon nanotube (Liu et al., 2008), MWCNTs (Salimi et al., 2004), and highly ordered mesoporous carbon foams (Zhou et al., 2008b).

On the other hand, the apparent Michalis–Menten constant (K_m), an indicator of enzyme–substrate reaction kinetics, is used to evaluate the biological activity of the immobilized enzyme, which can be calculated using the Lineweaver–Burk equation (Kamin and Wilson, 1980):

$$\frac{1}{I_{ss}} = \frac{1}{I_{max}} + \frac{K_m \cdot C_{glucose}}{I_{max}} \quad (1)$$

where I_{ss} is the steady-state response current after the addition of substrate, I_{max} is the maximum current under saturated substrate conditions, and $C_{glucose}$ is the bulk concentration of glucose. In this work, K_m of the G–CdS–GOD modified electrode is estimated to be 1.6 mM, which is smaller than those obtained from GOD–CdS (5.1 mM) (Huang et al., 2005), Nafion–GOD–SWCNTs (8.5 mM) (Liu et al., 2008) and graphene–chitosan–GOD modified substrate (4.4 mM) (Kang et al., 2009). The smaller K_m value indicates that the immobilized GOD possesses higher enzymatic activity and the G–CdS–GOD modified electrode exhibits a higher affinity for glucose than that reported (Kang et al., 2009; Huang et al., 2005), indicating that the G–CdS nanocomposite provides favorable microenvironment for GOD to perform the direct electron transfer at the modified electrode.

3.5. Interference

The interferences of electroactive species to the glucose response were examined in the presence of their physiological normal levels (Wang et al., 2005) with glucose concentration at 5.0 mM. The results show that addition of 0.5 mM uric acid and 0.1 mM ascorbic acid did not cause any interference to the G–CdS–GOD/GCE response to glucose, and 0.1 mM acetaminophen caused an increase of 4.7% in the reduction current of 5.0 mM glucose, which can be explained that the Nafion film can prevent them from diffusing through the film to the electrode surface (Dong and Kuwana, 1991). Thus, the proposed glucose biosensor can eliminate the interference of other coexisted electroactive substances such as ascorbic acid, uric acid and acetaminophen in blood by electro-reduction method.

3.6. Reproducibility and long-term stability of the biosensor

The reproducibility of the glucose biosensor was investigated by successively detecting 5.0 mM glucose for 6 times, the relative standard deviation (RSD) was 5.3%, demonstrating a good reproducibility. After 30 successively scanning the steady-state current was still retained 92% of its initial response, suggesting the acceptable durability of the biosensors. In addition, the RSD of current signals for measurement of 5.0 mM glucose at five independently prepared biosensors was 4.2%, which proved good reproducibility of the as-prepared biosensor.

The long-term storage stability is a critical issue for practical application of the proposed glucose biosensor. When stored in 0.05 M PBS at 4 °C and measured at intervals over 2 days, no obvious decrease in the response to glucose was observed after one week of storage. After 30 days the voltammetric response was still retained 93% value of the initial response. This implied that the G–CdS nanocomposite film was very efficient for retaining the bioactivity of enzyme and preventing its leakage from the membrane (Deng et al., 2009).

3.7. Determination of glucose in human plasma sample

In order to investigate the possible application of this biosensor in clinical analysis, the G–CdS–GOD modified electrode has been employed to the detection of blood sugar concentration in human plasma utilizing standard addition method without sample pretreatment. The concentration of glucose was determined to be 4.9 mM, and the recovery tests were performed by adding 1.0 and 2.0 mM glucose to the sample. The corresponding results were listed in Table 1 (Supplemental Information), and it can be obtained that the recoveries for the determination of glucose are between 92.2% and 105.1%. The result demonstrated good accuracy for the glucose sensing in real samples, ascertaining the practical application of the proposed glucose biosensor in clinical analysis.

4. Conclusions

In this paper, G–CdS nanocomposite can provide a unique microenvironment for the direct electrochemistry of GOD, and the immobilized GOD on the modified electrode possesses its native structure and electrocatalytic activities. The performance of the resulting electrode was improved greatly compared with that of GC electrode modified by graphene or CdS NCs alone by virtue of the synergy effect. Based on the decrease of the electrocatalytic response of the reduced form of GOD to dissolved oxygen, a glucose sensor has been developed, which displays satisfactory analytical performance over a linear range from 2.0 to 16 mM along with good stability because of the large surface area and fast electron transfer of graphene and CdS nanocrystals. Interference from uric acid and ascorbic acid that usually coexist with glucose in real samples has been found to be negligible. All these characteristics suggest that G–CdS nanocomposites are good materials for immobilizing biomolecules and fabricating the third-generation biosensors.

Acknowledgements

The present work is supported by the National Natural Science Foundation of China (Nos. 20875039 and 21075054), the Scientific Research Foundation of Jiangsu University (No. 06JDG016); Key Laboratory of Analytical Chemistry for Life Science (No. KLACLS07004); Key Laboratory of Modern Agriculture Equipment and Technology (No. NZ200809).

Appendix A. Supplementary data

Supplementary data associated with this article can be found, in the online version, at doi:10.1016/j.bios.2010.09.043.

References

Allen, M.J., Tung, V.C., Kaner, R.B., 2010. Chem. Rev. 110, 132–145.
Ang, P.K., Chen, W., Wee, A.T.S., Loh, K.P., 2008. J. Am. Chem. Soc. 130, 14392–14393.
Ao, Z.M., Yang, J., Li, S., Jiang, Q., 2008. Chem. Phys. Lett. 461, 276–279.
Bao, S.J., Li, C.M., Zang, J.F., Cui, X.Q., Qiao, Y., Guo, J., 2008. Adv. Funct. Mater. 18, 591–599.
Cao, A.N., Liu, Z., Chu, S.S., Wu, M.H., Ye, Z.M., Cai, Z.W., Chang, Y.L., Wang, S.F., Gong, Q.H., Liu, Y.F., 2009. Adv. Mater. 21, 1–4.
Dai, Z.H., Bai, H.Y., Hong, M., Zhu, Y.Y., Bao, J.C., Shen, J., 2008. Biosens. Bioelectron. 23, 1869–1873.
Deng, C.Y., Chen, J.H., Chen, X.L., Xiao, C.H., Nie, L.H., Yao, S.Z., 2008. Biosens. Bioelectron. 23, 1272–1277.
Deng, S.Y., Jian, G.Q., Lei, J.P., Hu, Z., Ju, H.X., 2009. Biosens. Bioelectron. 25, 373–377.
Dong, S.J., Kuwana, T., 1991. Electroanalysis 3, 485–591.
Geim, A.K., Novoselov, K.S., 2007. Nat. Mater. 6, 183–191.
Guo, P., Song, H.H., Chen, X.H., 2009. Electrochem. Commun. 11, 1320–1324.
Huang, Y.X., Zhang, W.J., Xiao, H., Li, G.X., 2005. Biosens. Bioelectron. 21, 817–821.
Kamin, R.A., Wilson, G.S., 1980. Anal. Chem. 52, 1198–1205.
Kang, X.H., Wang, J., Wu, H., Aksay, I.A., Liu, J., Lin, Y.H., 2009. Biosens. Bioelectron. 25, 901–905.
Kim, Y.R., Bong, S., Kang, Y.J., Yang, Y., Mahajan, R.K., Kim, J.S., Kim, H., 2010. Biosens. Bioelectron. 25, 2366–2369.
Laviron, E., 1979. J. Electroanal. Chem. 101, 19–28.
Li, D., Müller, M.B., Gilje, S., Kaner, R.B., Wallace, G.G., 2008. Nat. Nanotechnol. 3, 101–105.
Li, J., Guo, S.J., Zhai, Y.M., Wang, E.K., 2009a. Electrochem. Commun. 11, 1085–1088.
Li, F.H., Song, J.X., Li, F., Wang, X.D., Zhang, Q.X., Han, D.X., Ivaska, A., Niu, L., 2009b. Biosens. Bioelectron. 25, 883–888.
Liu, S.Q., Ju, H.X., 2003. Biosens. Bioelectron. 19, 177–183.
Liu, Y., Wang, M.K., Zhao, F., Xu, Z.A., Dong, S.J., 2005. Biosens. Bioelectron. 21, 984–988.
Liu, Y., Yuan, R., Chai, Y.Q., Tang, D.P., Dai, J.Y., Zhong, X., 2006. Sens. Actuators B 115, 109–115.
Liu, Q., Lu, X.B., Li, J., Yao, X., Li, J.H., 2007. Biosens. Bioelectron. 22, 3203–3209.
Liu, X.Q., Shi, L.H., Niu, W.X., Li, H.J., Xu, G.B., 2008. Biosens. Bioelectron. 23, 1887–1890.
Luo, X., Killard, A.J., Smyth, M.R., 2006. Electroanalysis 18, 1131–1134.
Salimi, A., Compton, R.G., Hallaj, R., 2004. Anal. Biochem. 333, 49–56.
Shan, C.S., Yang, H.F., Song, J.F., Han, D.X., Ivaska, A., Niu, L., 2009. Anal. Chem. 81, 2378–2382.
Shan, C.S., Yang, H.F., Han, D.X., Zhang, Q.X., Ivaska, A., Niu, L., 2010. Biosens. Bioelectron. 25, 1070–1074.
Shao, Y.Y., Wang, J., Wu, H., Liu, J., Aksay, I.A., Lin, Y.H., 2010. Electroanalysis 22, 1027–1036.
Stankovich, S., Dikin, D.A., Dommett, G.H.B., Kohlhaas, K.M., Zimney, E.J., Stach, E.A., Piner, R.D., Nguyen, S.T., Ruoff, R.S., 2006. Nature 442, 282–286.
Stoller, M.D., Park, S.J., Zhu, Y.W., An, J.H., Ruoff, R.S., 2008. Nano Lett. 8, 3498–3502.
Wang, K., Xu, J.J., Chen, H.Y., 2005. Biosens. Bioelectron. 20, 1388–1396.
Wang, X., Zhi, L.J., Müllen, K., 2008. Nano Lett. 8, 323–327.
Wang, D.H., Choi, D.W., Li, J., Yang, Z.G., Nie, Z.M., Kou, R., Hu, D.H., Wang, C.M., Saraf, L.V., Zhang, J.G., Aksay, I.A., Liu, J., 2009a. ACS Nano 3, 907–914.
Wang, K.Q., Yang, H., Zhu, L., Liao, J.H., Lu, T.H., Xing, W., Xing, S.Y., Lv, Q., 2009b. J. Mol. Catal. B: Enzym. 58, 194–198.
Wang, Y., Li, Y.M., Tang, L.H., Lu, J., Li, J.H., 2009c. Electrochem. Commun. 11, 889–892.
Wang, Y., Wan, Y., Zhang, D., 2010a. Electrochem. Commun. 12, 187–190.
Wang, K., Liu, Q., Wu, X.Y., Guan, Q.M., Li, H.N., 2010b. Talanta 82, 372–376.
Wen, D., Liu, Y., Yang, G.C., Dong, S.J., 2007. Electrochim. Acta 52, 5312–5317.
Wu, S., Ju, H.X., Liu, Y., 2007. Adv. Funct. Mater. 17, 585–592.
Wu, H., Wang, J., Kang, X.H., Wang, C.M., Wang, D.H., Liu, J., Aksay, I.A., Lin, Y.H., 2009. Talanta 80, 403–406.
Wu, J.F., Xu, M.Q., Zhao, G.C., 2010. Electrochem. Commun. 12, 175–177.
Yang, M.H., Jiang, J.H., Yang, Y.H., Chen, X.H., Shen, G.L., Yu, R.Q., 2006. Biosens. Bioelectron. 21, 1791–1797.
Zhao, S., Zhang, K., Bai, Y., Yang, W.W., Sun, C.Q., 2006. Bioelectrochemistry 69, 158–163.
Zhao, H.Z., Sun, J.J., Song, J., Yang, Q.Z., 2010. Carbon 48, 1508–1514.
Zhou, Y., Yang, H., Chen, H.Y., 2008a. Talanta 76, 419–423.
Zhou, M., Shang, L., Li, B.L., Huang, L.J., Dong, S.J., 2008b. Biosens. Bioelectron. 24, 442–447.
Zou, Y.J., Sun, L.X., Xu, F., 2007. Biosens. Bioelectron. 22, 2669–2674.